Electronic Supplementary Information

An asymmetrical fused-ring electron acceptor designed by a cross-conceptual strategy achieving 15.6% efficiency

Wei Gao,[ac] Xiaoling Ma,[b] Qiaoshi An,[b] Jinhua Gao,[b] Cheng Zhong,[c] Fujun Zhang*[b] and Chuluo Yang*[ac]

[a]Shenzhen Key Laboratory of Polymer Science and Technology, College of Materials Science and Engineering, Shenzhen University, Shenzhen 518060, People's Republic of China
[b]Key Laboratory of Luminescence and Optical Information, Ministry of Education, Beijing Jiao tong University, Beijing, 100044, People's Republic of China
[c]Department of Chemistry, Hubei Key Lab on Organic and Polymeric Optoelectronic Materials, Wuhan University, Wuhan, 430072, People's Republic of China

General information

All solvents and reagents were used as received from commercial sources and used without further purification except for toluene which were dried by potassium sodium alloy under refluxing condition. ^{1}H NMR and ^{13}C NMR spectra were recorded on a Bruker Advanced II (400 MHz) spectrometer. The high-resolution mass spectra (HRMS) and matrix-assisted laser desorption/ionization time of flight mass spectrometry (MALDI-TOF-MS) were performed on Thermo Scientific LTQ Orbitrap Xl using ESI and 5800 MALDI-TOF/TOF mass spectrometry (AB SCIEX, USA) in positive mode, respectively. UV-vis spectra were measured using a Shimadzu UV-2500 recording spectrophotometer. Cyclic voltammetry (CV) measurements of targeted SMAs thin films were conducted on a CHI voltammetric analyzer in acetonitrile solution with 0.1 M tetrabutylammonium hexafluorophosphate (n-Bu_4NPF_6) as supporting electrolyte at room temperature by using a scan rate of 100 mV s^{-1} and conventional three-electrode configuration. Transmission electron microscopy (TEM) images of the active layers were obtained by using a JEOL JEM-1400 transmission electron microscope operated at 80 kV.

Synthesis

IT6-4F and Y6 were synthesized according to reported methods.[1,2] 4,7-dibromo-5,6-

dinitrobenzo[*c*][1,2,5]thiadiazole (compound **1**), tributyl(6-undecylthieno[3,2-*b*]thiophen-2-yl)stannane, tributyl(4-hexylthiophen-2-yl)stannane and 2-(5,6-difluoro-3-oxo-2,3-dihydro-1*H*-inden-1-ylidene)malononitrile were purchased from Hyper and Derthon.

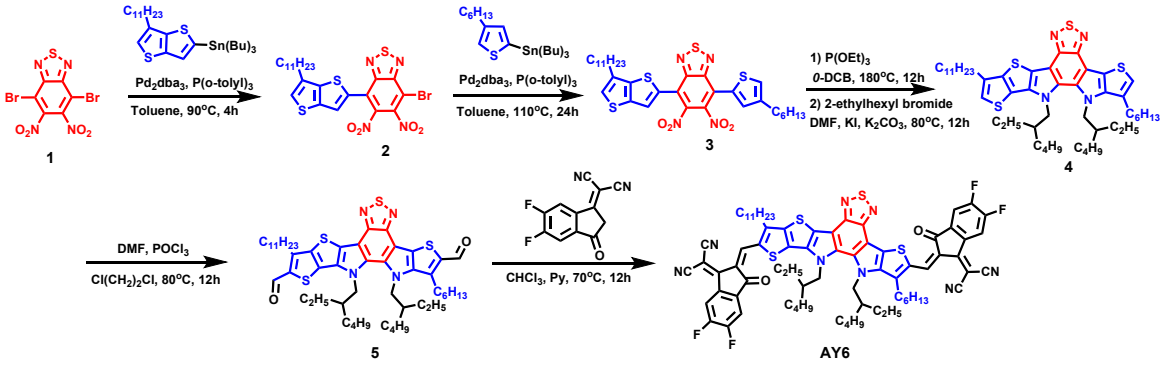

Scheme S1. The synthetic routes of AY6.

Synthesis of ***compound 2***: To a dry 100 ml round-bottom flask, compound **1** (1.0 g, 2.62 mmol), tributyl(6-undecylthieno[3,2-*b*]thiophen-2-yl)stannane (1.22 g, 2.1 mmol), Pa_2dba_3 (36 mg, 0.04 mmol), P(*o*-tolyl)$_3$ (48 mg, 0.16 mmol) and anhydrous toluene (50 ml) was added under argon protection. Then, the mixture was refluxed at 90°C for 4h. After cooling to room temperature, the solvent was evaporated and the residue was purified by silicon chromatography using petroleum ether/dichloromethane (5:1, v/v) as eluent to get the product as a red solid (525 mg, 42%). ^{1}H NMR (400 MHz, $CDCl_3$), δ (ppm): 7.68 (s, 1H), 7.18 (s, 1H), 2.76 (t, J_1 = 8.0 Hz, 2H), 1.73-1.81 (m, 2H), 1.26-1.40 (m, 16H), 0.87 (t, J = 6.4 Hz, 3H). ^{13}C NMR (100 MHz, $CDCl_3$), δ (ppm): 152.38, 151.36, 151.21, 144.43, 139.14, 135.13, 129.36, 125.48, 124.38, 122.74, 110.32, 108.62, 31.94, 29.81, 29.68, 29.66, 29.60, 29.39, 29.38, 28.56, 22.72, 14.17. HRMS (ESI) m/z calcd for $C_{23}H_{26}BrN_4O_4S_3^+$ $(M+H)^+$ 597.02941, found 597.02917.

Synthesis of ***compound 3***: To a dry 100 ml round-bottom flask, compound **2** (500 mg, 0.84 mmol), tributyl(4-hexylthiophen-2-yl)stannane (461 mg, 1.0 mmol), Pa_2dba_3 (36 mg, 0.04 mmol), P(*o*-tolyl)$_3$ (48 mg, 0.16 mmol) and anhydrous toluene (30 ml) was added under argon protection. Then, the mixture was refluxed at 110°C for 24h. After cooling to room temperature, the solvent was evaporated and the residue was purified

by silicon chromatography using petroleum ether/dichloromethane (4:1, v/v) as eluent to get the product as a red solid (530 mg, 92%). ^{1}H NMR (400 MHz, $CDCl_3$), δ (ppm): 7.68 (s, 1H), 7.33 (s, 1H), 7.32 (s, 1H), 7.16 (s, 1H), 2.74-2.78 (m, 2H), 2.64-2.69 (m, 2H), 1.76-1.80 (m, 2H), 1.63-1.68 (m, 2H), 1.26-1.40 (m, 22H), 0.86-0.91 (m, 6H). ^{13}C NMR (100 MHz, $CDCl_3$), δ (ppm): 152.22, 152.17, 152.13, 144.48, 144.42, 144.13, 141.79, 141.57, 139.03, 135.10, 132.23, 132.16, 130.08, 129.20, 126.64, 126.46, 125.10, 124.02, 121.62, 121.38, 121.19, 31.95, 31.67, 30.34, 30.27, 29.85, 29.70, 29.67, 29.61, 29.42, 29.39, 28.92, 28.58, 22.73, 22.64, 14.18, 14.15. HRMS (ESI) m/z calcd for $C_{33}H_{41}N_4O_4S_4^+$ $(M+H)^+$ 685.20052, found 685.20074.

Synthesis of ***compound 4***: To a dry 25 ml round-bottom flask, compound **3** (515 mg, 0.75 mmol), triethyl phosphite (1 ml) and anhydrous *o*-dichlorobenzene (10 ml) was added under argon protection. Then, the mixture was heated to 180^{o}C and kept stirring for 12h. After cooling to room temperature, the solvent was evaporated under reduced pressure. Without further purification, potassium iodide (66 mg, 0.4 mmol), potassium carbonate (415 mg, 3 mmol) 2-ethylhexyl bromide (865 mg, 4.5 mmol) and *N*,*N*-dimethylformamide (10 ml) were added into the residue. The mixture was kept stirring at 80^{o}C for 12h. After cooling to room temperature, the mixture was extracted with dichloromethane and washed with water. The collected organic layer was dried over anhydrous Na_2SO_4 and concentrated. The residue was purified by silicon chromatography using petroleum ether/dichloromethane (6:1, v/v) as eluent to get the product as a yellow solid (427 mg, 67%). ^{1}H NMR (400 MHz, $CDCl_3$), δ (ppm): 7.05 (s, 1H), 7.01 (s, 1H), 4.61 (d, J = 6.8 Hz, 2H), 4.48 (d, J = 7.2 Hz, 2H), 2.92 (t, J = 7.6 Hz, 2H), 2.82 (t, J = 7.6 Hz, 2H), 1.98-2.01 (m, 1H), 1.82-1.89 (m, 4H), 1.72-1.75 (m, 1H), 0.57-1.50 (m, 56H). ^{13}C NMR (100 MHz, $CDCl_3$), δ (ppm): 147.74, 147.70, 143.71, 142.02, 136.85, 136.81, 134.91, 131.89, 128.65, 123.62, 123.28, 122.28, 119.27, 111.30, 110.61, 54.36, 53.73, 40.56, 39.99, 31.96, 31.80, 29.79, 29.72, 29.67, 29.64, 29.54, 29.50, 29.39, 29.33, 29.22, 28.83, 22.79, 22.73, 22.66, 14.17, 14.15, 13.70. HRMS (ESI) m/z calcd for $C_{49}H_{73}N_4S_4^+$ $(M+H)^+$ 845.47126, found 845.47150.

Synthesis of ***compound 5***: To a dry 50 ml two-necked round bottom flask, 5 ml anhydrous *N*, *N*-dimethylformamide (DMF) was added, and the solution was cooled to 0°C and stirred when 1 ml phosphorous oxychloride ($POCl_3$) was added by syringe under argon protection. The mixture was stirred at 0°C for 1 hour, and then compound **4** (420 mg, 0.50 mmol) in dry 1, 2-dichloroethane (10 ml) was added. Then, the mixture solution was allowed reflux overnight. After cooling to room temperature, 100 ml water was added and the mixture was extracted with dichloromethane (DCM), and the organic layer was collected, washed with water and dried with anhydrous Na_2SO_4. After removal of the solvent under reduced pressure, the residue was purified by column chromatography on silica gel using a mixture solvent as eluent (petroleum ether/dichloromethane, v/v = 1/1) to give an orange solid (370 mg, 83%). ^{1}H NMR (400 MHz, $CDCl_3$), δ (ppm): 10.16 (s, 1H), 10.15 (s, 1H), 4.65 (d, *J* = 7.2 Hz, 2H), 4.51 (d, *J* = 7.2 Hz, 2H), 3.19-3.23 (m, 4H), 1.89-1.97 (m, 5H), 1.70-1.75 (m, 1H), 0.66-1.51 (m, 56H). ^{13}C NMR (100 MHz, $CDCl_3$), δ (ppm): 182.35, 181.92, 147.57, 146.98, 144.09, 143.54, 139.20, 137.63, 137.34, 132.64, 130.54, 129.47, 127.62, 113.03, 111.24, 54.53, 54.15, 40.87, 40.18, 31.91, 31.69, 31.54, 30.34, 29.72, 29.64, 29.61, 29.52, 29.38, 29.34, 29.15, 28.18, 27.12, 22.70, 22.55, 14.15, 14.09, 13.62. HRMS (ESI) m/z calcd for $C_{51}H_{73}N_4O_2S_4^+$ $(M+H)^+$ 901.46109, found 901.46057.

Synthesis of ***AY6***: To a 100 ml round bottom flask, compound **5** (150 mg, 0.167 mmol) and 2-(5,6-difluoro-3-oxo-2,3-dihydro-1*H*-inden-1-ylidene)malononitrile (154 mg, 0.67 mmol) were added under argon protection. Then, deoxidized chloroform (40 ml) was added and stirred for a while when pyridine (1 ml) was added. The mixture was kept stirring at 70°C for 12 h. After removal of chloroform of reaction mixture under reduced pressure, 100 ml methanol was added and the precipitate was collected by filtration. The residue was purified by column chromatography on silica gel using a mixture solvent as eluent (petroleum ether/dichloromethane, v/v = 2/1) to give a dark solid (197 mg, 89%). ^{1}H NMR (400 MHz, $CDCl_3$), δ (ppm): 9.20 (s, 1H), 9.14 (s, 1H), 8.54-8.58 (m, 2H), 7.68-7.72 (m, 2H), 4.78 (d, *J* = 6.0 Hz, 2H), 4.57 (s, 2H), 3.20 (m, 4H), 2.03 (m, 1H), 1.78-1.88 (m, 5H), 0.71-1.60 (m, 54H). ^{13}C NMR (100 MHz,

$CDCl_3$), δ (ppm): 186.11, 185.66, 159.41, 158.73, 155.74, 155.50, 153.75, 153.12, 152.98, 147.60, 147.55, 145.65, 145.59, 145.27, 143.69, 140.13, 138.71, 138.18, 136.59, 136.39, 135.70, 135.61, 135.46, 135.24, 134.56, 134.34, 133.57, 133.44, 130.82, 120.43, 120.36, 115.28, 115.07, 114.95, 114.84, 114.74, 114.48, 112.66, 112.47, 112.11, 69.16, 68.14, 55.04, 54.36, 32.18, 31.92, 31.79, 31.19, 29.82, 29.65, 29.62, 29.51, 29.44, 29.35, 29.27, 28.12, 22.81, 22.69, 22.55, 14.14, 14.12, 13.73. MALDI-TOF-MS m/z: [M] calcd. for $C_{75}H_{76}F_4N_8O_2S_4$, 1324.49, found 1324.11.

Devices fabrication and characterization

The conventional photovoltaic devices were fabricated with a structure of ITO/PEDOT:PSS/PM6:acceptor/PDIN/Al. First, the patterned ITO-coated glass with a sheet resistance of 15 Ω sq^{-1} was scrubbed by detergent and then cleaned inside an ultrasonic bath by using deionized water, acetone, and isopropyl alcohol sequentially. The ITO substrate was fast dried by using high pure nitrogen gas and then treated by oxygen plasma for 1 min to improve its work function and clearance. Then, PEDOT:PSS (Heraeus Clevios P VP A 4083) layer was spin-coated onto ITO substrate with a thickness of about 40 nm and dried at 150°C for 10 minutes in air, and the PEDOT:PSS coated ITO substrates were fast transferred to a N_2 filled glove-box for further processing. The blend solution (with 0.5% CN, v/v) in chloroform (CF) with a total concentration of 16 mg/ml (PM6:acceptor (wt/wt:1:1.2)) was drop-cast at the PEDOT:PSS layer at 2500 rpm for 1 min and controlled the active layer thickness of ~110 nm measured by Ambios Technology XP-2 stylus Profiler. After spin-coated, the active layer was fumigated by CS_2 for 30 s and then annealed at 100°C for 3 minutes. Next, the methanol solution of PDIN of 1.0 mg/ml was deposited atop the active layer at 3000 rpm for 30 s to afford a PDIN cathode buffer layer with thickness of ca. 10 nm. Subsequently, the active layer coated substrates were quickly transferred to a glove-box integrated thermal evaporator for Al deposition. Al (100 nm) layers were evaporated onto the active layer through a shadow mask at a vacuum pressure of ≈ 5×10^{-5} Pa to form top electrode. The active area of cells is 3.8 mm^2, which is defined by the vertical overlap of ITO cathode and Al anode. The current-voltage (*J-V*) characteristic curves

of all devices were measured by using a Keithley 2400 Source Meter in a high-purity nitrogen-filled glove box. AM 1.5G irradiation at 100 mW/cm^2 provided by a XES-40S2 (SAN-EI Electric Co., Ltd.) solar simulator (AAA grade, 70×70 mm^2 photobeam size), which was calibrated by standard silicon solar cells (purchased from Zolix INSTRUMENTS CO. LTD). The external quantum efficiency (EQE) spectra of all devices were measured in air conditions by a Zolix Solar Cell Scan 100.

SCLC measurements

The structure of electron-only devices is ITO/ZnO/active layer/PDIN/Al and the structure of hole-only devices is ITO/PEDOT:PSS/active layer/MoO_3/Ag. The fabrication conditions of the active layer films are same with those for the PSCs. The charge mobilities are generally described by the Mott-Gurney equation:[3-5]

$$J = \frac{9}{8}\varepsilon_r\varepsilon_0\mu\frac{V^2}{L^3} \quad (1)$$

where J is the current density, ε_0 is the permittivity of free space (8.85 × 10^{-14} F/cm), ε_r is the dielectric constant of used materials, μ is the charge mobility, V is the applied voltage and L is the active layer thickness. The ε_r parameter is assumed to be 3, which is a typical value for organic materials. In organic materials, charge mobility is usually field dependent and can be described by the disorder formalism, typically varying with electric field, E=V/L, according to the equation:

$$\mu = \mu_0 \exp[0.89\gamma\sqrt{\frac{V}{L}}] \quad (2)$$

where μ_0 is the charge mobility at zero electric field and γ is a constant. Then, the Mott-Gurney equation can be described by[6-8]:

$$J = \frac{9}{8}\varepsilon_r\varepsilon_0\mu_0\frac{V^2}{L^3}\exp[0.89\gamma\sqrt{\frac{V}{L}}] \quad (3)$$

In this case, the charge mobilities were estimated using the following equation:

$$\ln(\frac{JL^3}{V^2}) = 0.89\gamma\sqrt{\frac{V}{L}} + \ln(\frac{9}{8}\varepsilon_r\varepsilon_0\mu_0) \quad (4)$$

GIWAXS characterization

The GIWAXS characterization were performed at BL16B1 beamline of Shanghai Synchrotron Radiation Facility. The samples were prepared under the same conditions of the OSCs on the Glass/PEDOT:PSS substrates. The wavelength of incident X-ray was 0.124 nm and the exposure time of samples was 60 s. The incidence light angle of X ray was 0.12° and the scattering signal was collected by mar165CCD with a pixel size of 0.172 mm by 0.172 mm. The sample-to-detector distance was ≈ 252 mm (calibrated by AgB sample). The GIWAXS characterization was done in air environment.

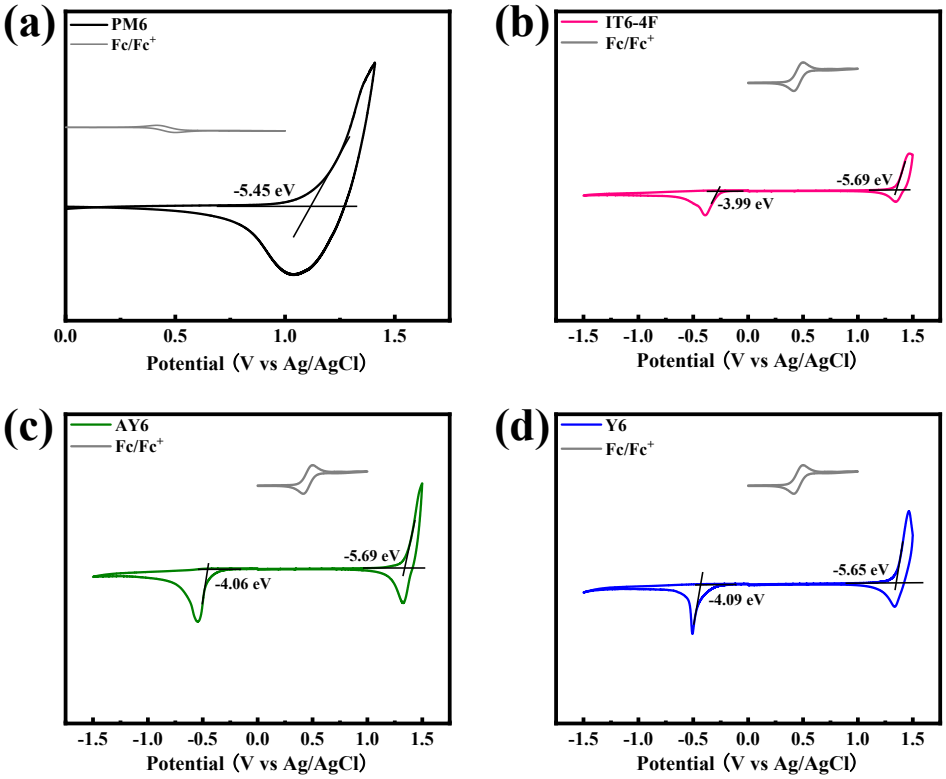

Fig. S1 The CV curves of PM6, IT6-4F, AY6 and Y6 neat films measured in acetonitrile.

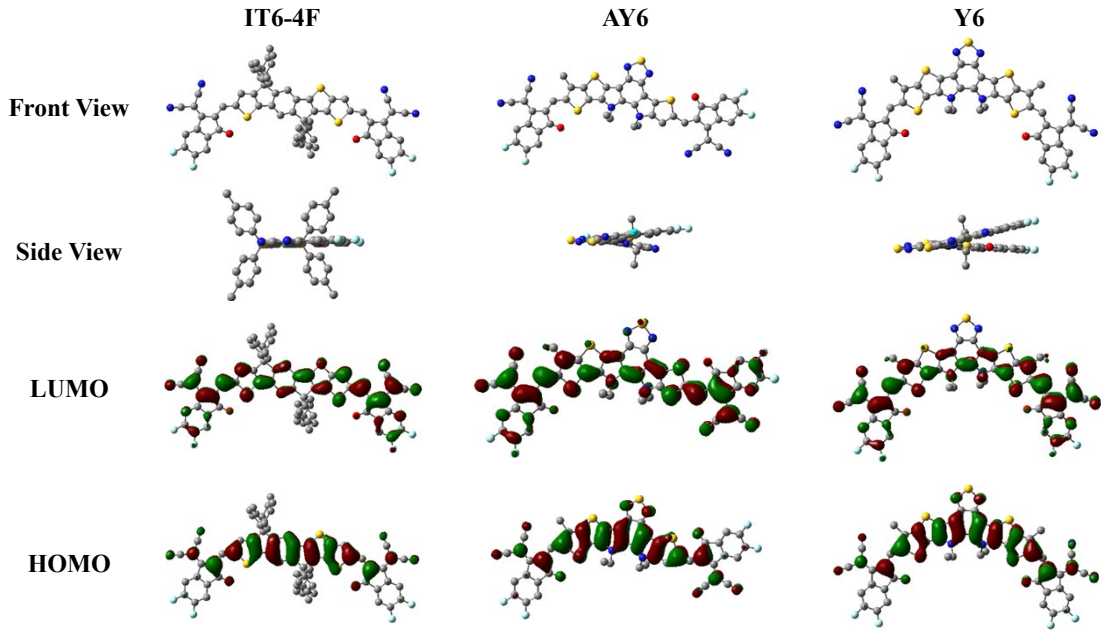

Fig. S2 DFT calculation results: the front view and side view of molecular backbone, and the HOMO and LUMO distribution for optimal IT6-4F, AY6 and Y6.

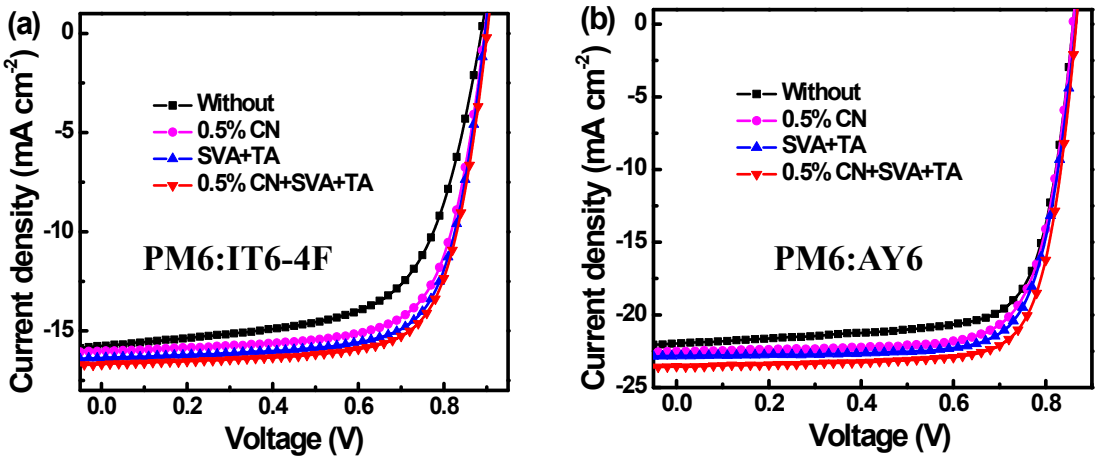

Fig. S3 The *J-V* curves of OSCs based on PM6:IT6-4F and PM6:AY6 with different treatments.

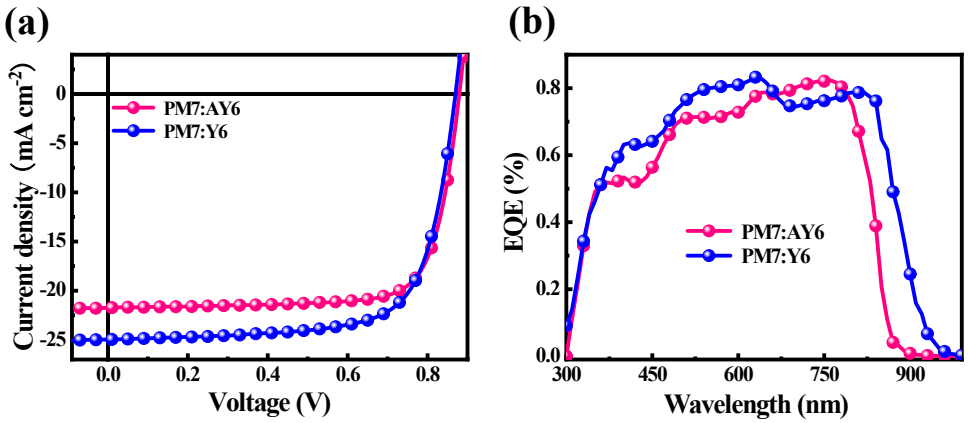

Fig. S4 *J-V* curves and EQE spectra of PM7:AY6- and PM7:Y6-based OSCs.

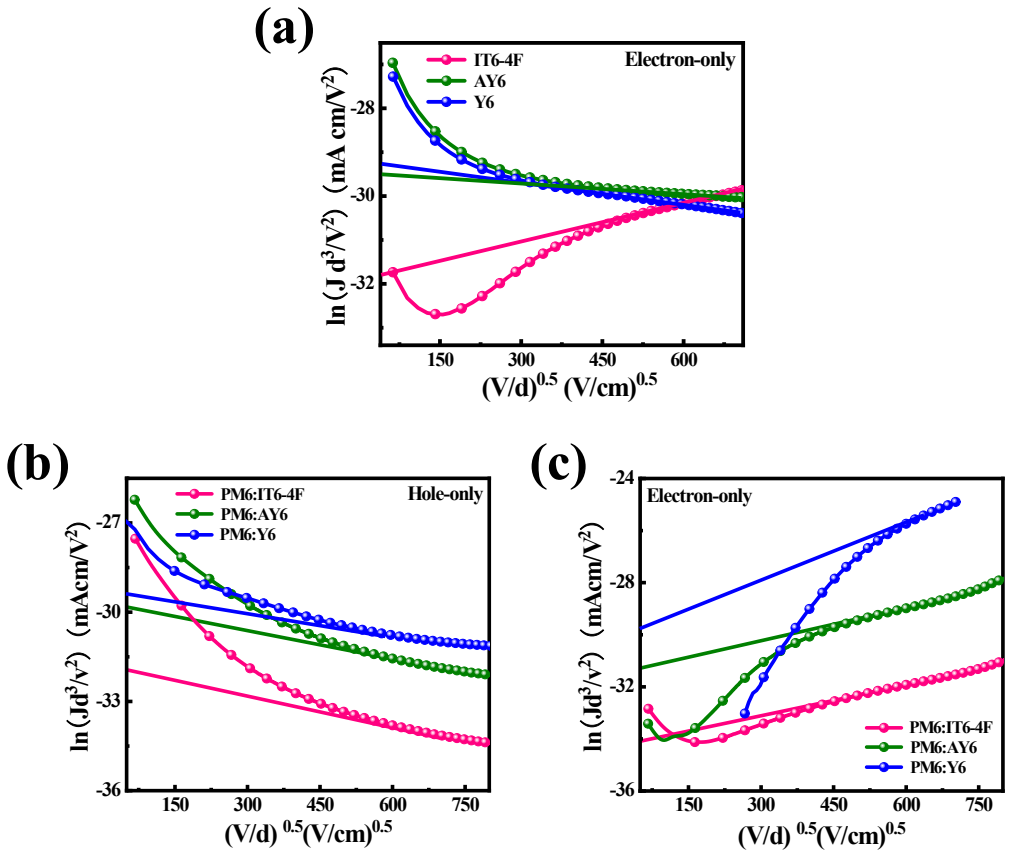

Fig. S5 The *J-V* curves of SCLC measurements for IT6-4F, AY6 and Y6 neat and blend films.

Table S1 Key photovoltaic parameters of OSCs based on PM6:IT6-4F and PM6:AY6 with different treatments.

Acceptor	Treatment	J_{SC} (mA cm^{-2})	V_{OC} (V)	FF (%)	PCE (%)
PM6:IT6-4F	—	15.75	0.89	63.33	8.62
	0.5% CN	16.02	0.89	70.84	10.10
	SVA+TA	16.37	0.90	71.66	10.56
	0.5% CN, SVA +TA	16.69	0.90	72.12	10.83
PM6:AY6	—	21.97	0.86	73.57	13.90
	0.5% CN	22.51	0.86	74.91	14.50
	SVA+TA	22.82	0.87	75.42	14.97
	0.5% CN, SVA +TA	23.54	0.87	76.24	15.61

Table S2 Optimal photovoltaic parameters of OSCs based on PM7:AY6 and PM6:Y6.

Active layer	V_{oc} (V)	J_{sc}[a] (mA cm^{-2})	FF (%)	PCE[b] (%)
PM7:AY6	0.880	21.73 (21.22)	76.5	14.6 (14.5 ± 0.1)
PM7:Y6	0.868	24.98 (24.44)	71.4	15.5 (15.4 ± 0.1)

[a]In brackets are integral J_{sc} from EQE; [b]In brackets are average values from ten devices.

Table S3 Summary of Key photovoltaic parameters of OSCs based on asymmetrical SMAs.

Active Layer	V_{oc} (V)	J_{sc} (mA cm^{-2})	FF (%)	PCE (%)	Ref.
PM6:AY6	0.87	23.54	76.3	15.6	This Work
PBDB-T:A102	0.96	9.66	60.9	5.65	6
PCE10:FPDI-Se	0.80	14.78	56.1	6.61	7
PBDB-T:IDT6CN-M	0.91	16.02	76.8	11.20	8
PBT1-C:TPTTT-2F	0.92	17.63	74.5	12.03	9
PBDB-T:IDT8CN-M	0.92	17.11	78.9	12.43	10
PBDB-T:MeIC1	0.93	18.32	74.1	12.58	11
PBT1-C:TTPTTT-4F	0.86	19.36	72.1	12.05	12
PBT1-C:SePTTT-2F	0.90	18.02	75.9	12.24	13
PBT1-C-2Cl:IDTT-2F-Th	0.91	17.82	73.9	12.01	14
PBDB-TF:ITIC-3F	0.89	19.4	66.5	11.44	15
PBDB-T:a-IT-2OM	0.93	18.11	71.5	12.07	16
PBDB-TF:IT-3F	0.90	20.35	75.5	13.83	17
J71:ZITI-3F	0.90	20.67	71.3	13.15	18
PM6:N7IT	0.93	21.04	70.5	13.82	19
PBDB-T:IPT-2F	0.86	22.4	72.4	14.0	20

Table S4 Hole and electron mobilities of five PM6:AY6- and PM6:Y6-based devices.

PM6:AY6	Hole (10^{-4} cm^2 V^{-1} s^{-1})	Electron (10^{-4} cm^2 V^{-1} s^{-1})
1	3.75	0.862
2	3.42	0.903
3	3.96	0.879
4	3.80	0.827
5	3.56	0.837
Average	3.70 ± 0.21	0.862 ± 0.03

PM6:Y6	Hole (10^{-4} cm^2 V^{-1} s^{-1})	Electron (10^{-4} cm^2 V^{-1} s^{-1})
1	6.12	1.25
2	5.79	1.27
3	6.35	1.18
4	5.98	1.03
5	6.13	1.34
Average	6.07 ± 0.21	1.21 ± 0.12

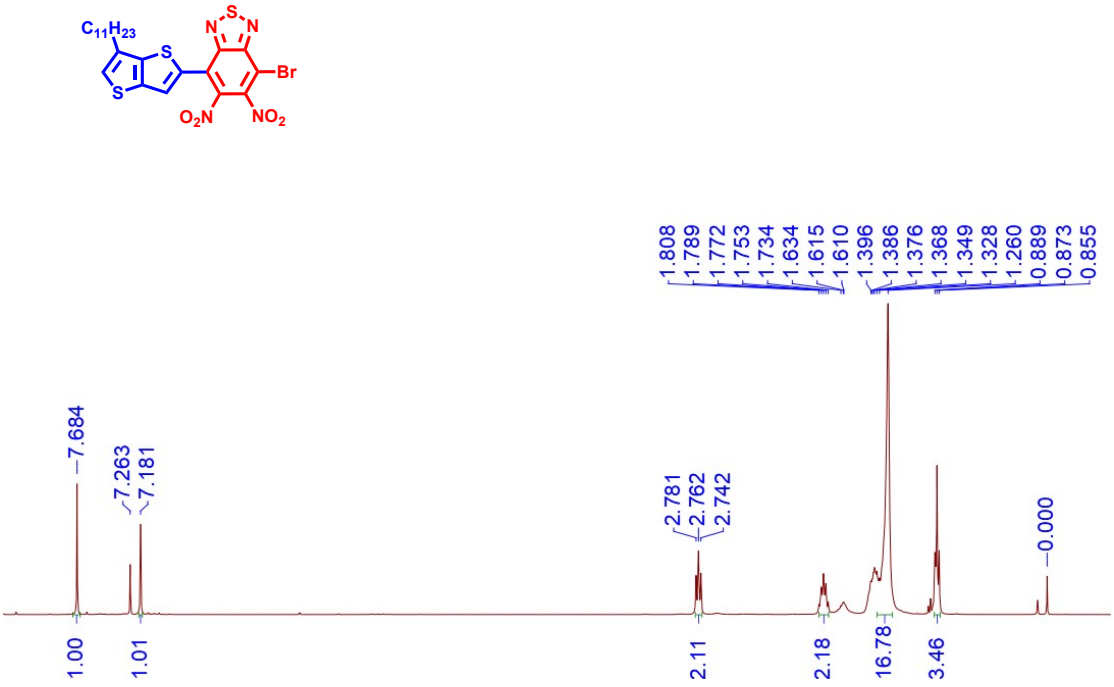

Fig. S6 The ^{1}H NMR spectrum of **Compound 2** in $CDCl_3$.

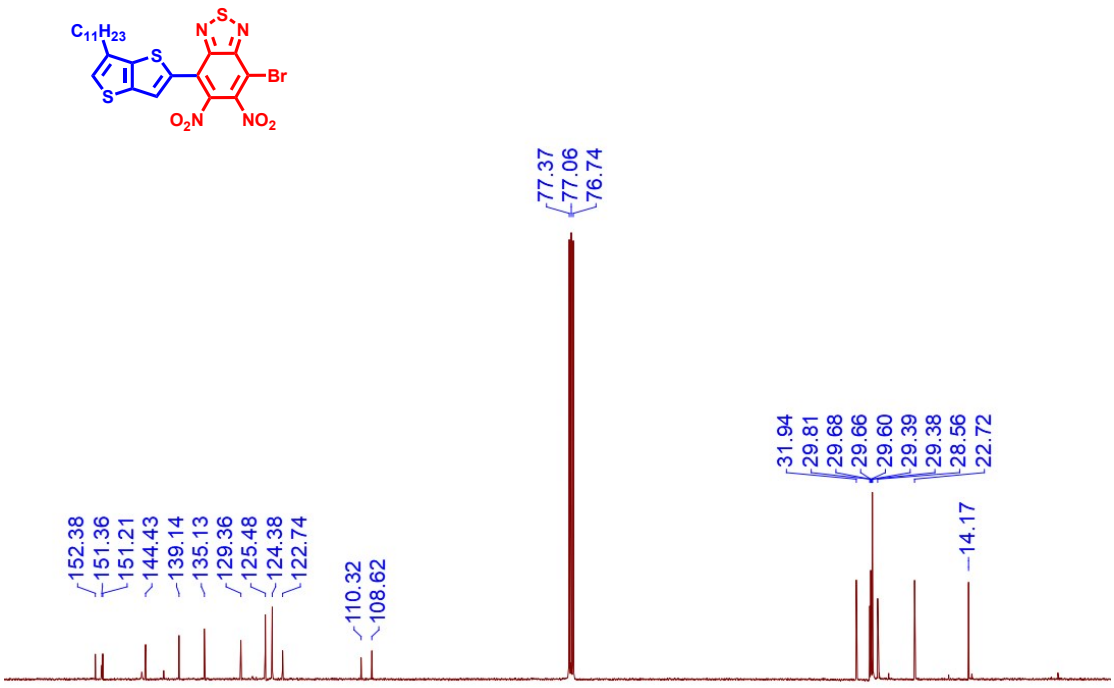

Fig. S7 The ^{13}C NMR spectrum of **Compound 2** in $CDCl_3$.

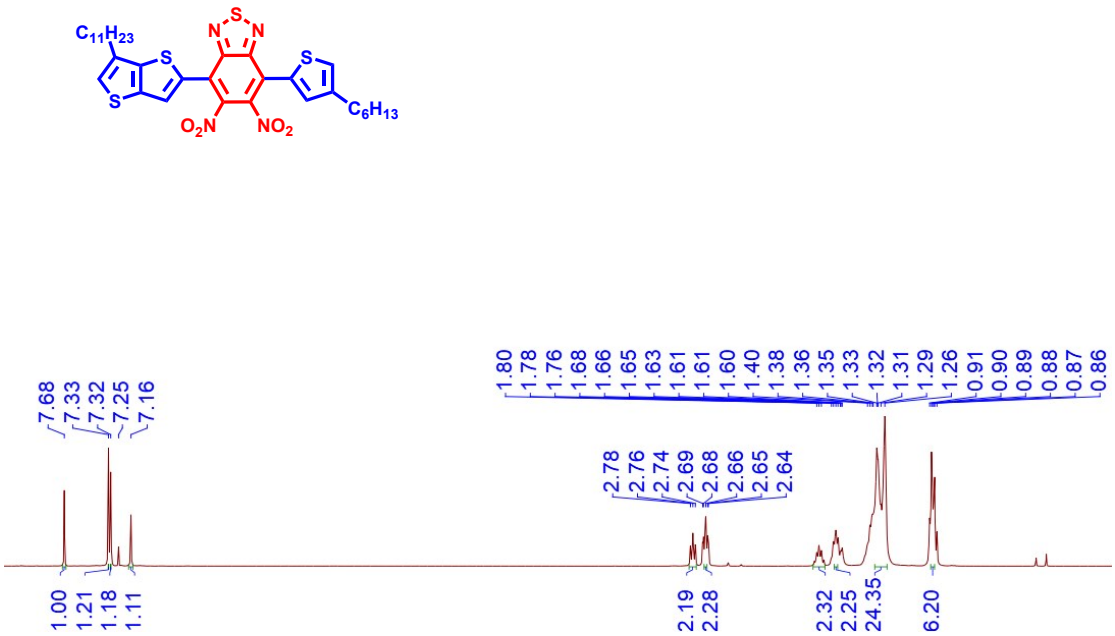

Fig. S8 The ^{1}H NMR spectrum of **Compound 3** in $CDCl_3$.

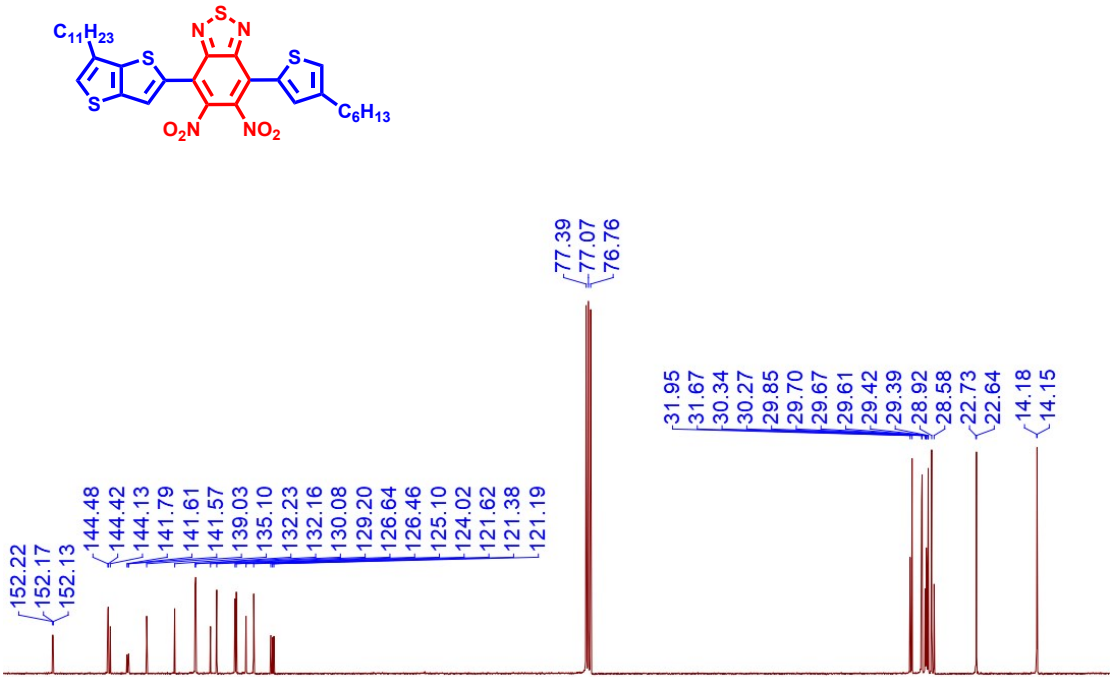

Fig. S9 The ^{13}C NMR spectrum of **Compound 3** in $CDCl_3$.

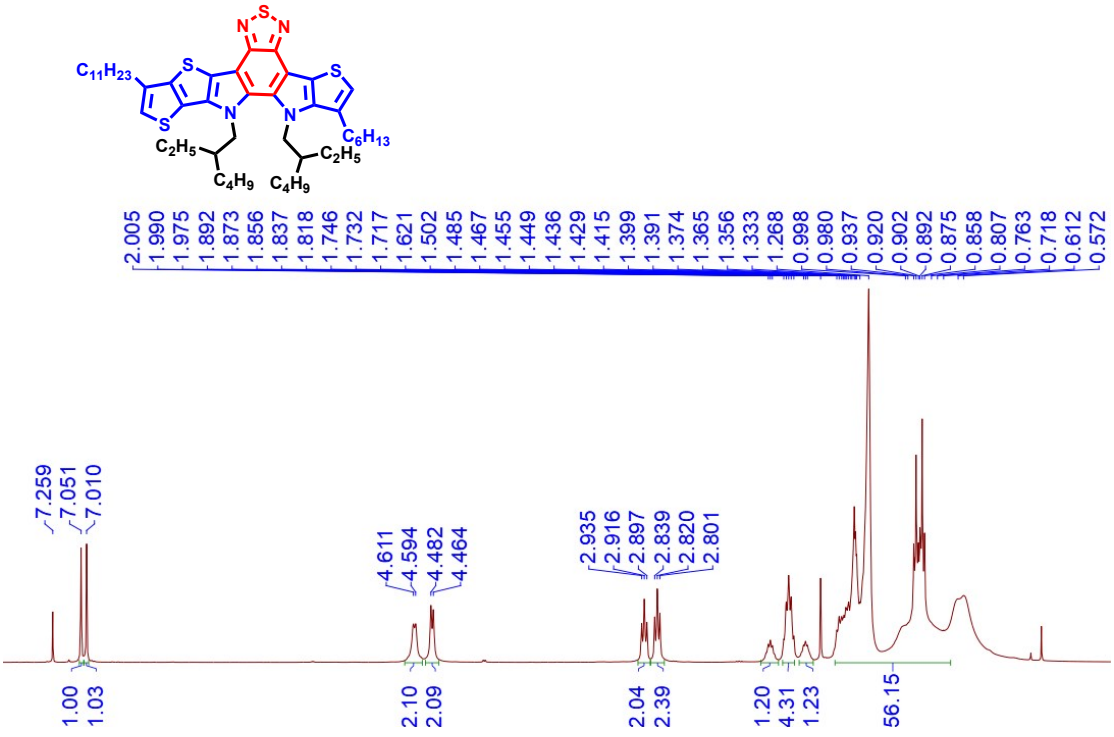

Fig. S10 The ^{1}H NMR spectrum of **Compound 4** in $CDCl_3$.

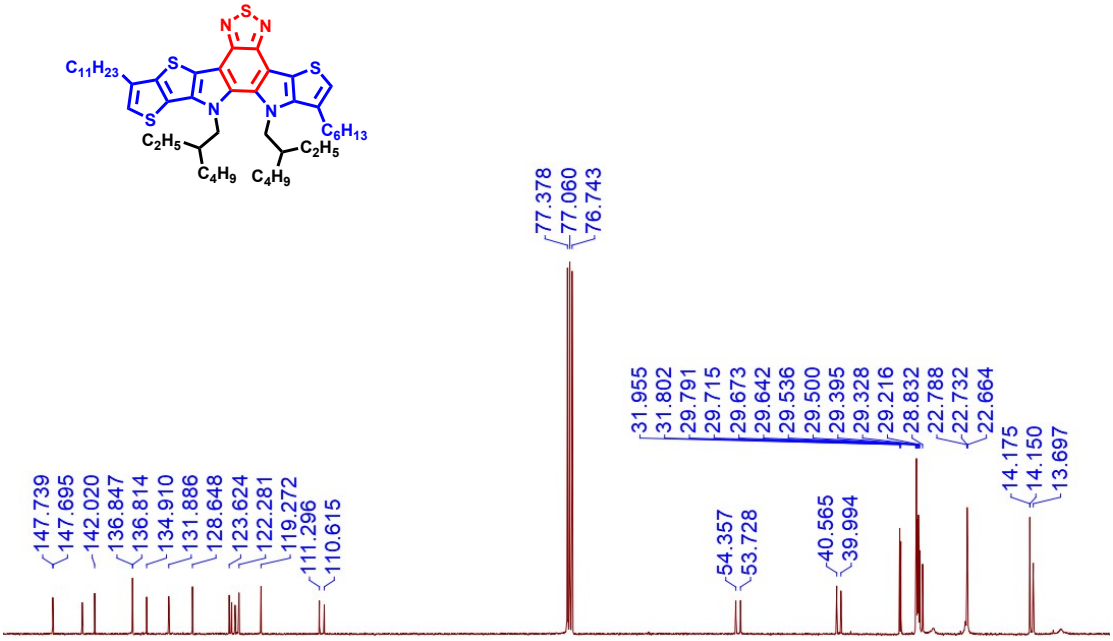

Fig. S11 The ^{13}C NMR spectrum of **Compound 4** in $CDCl_3$.

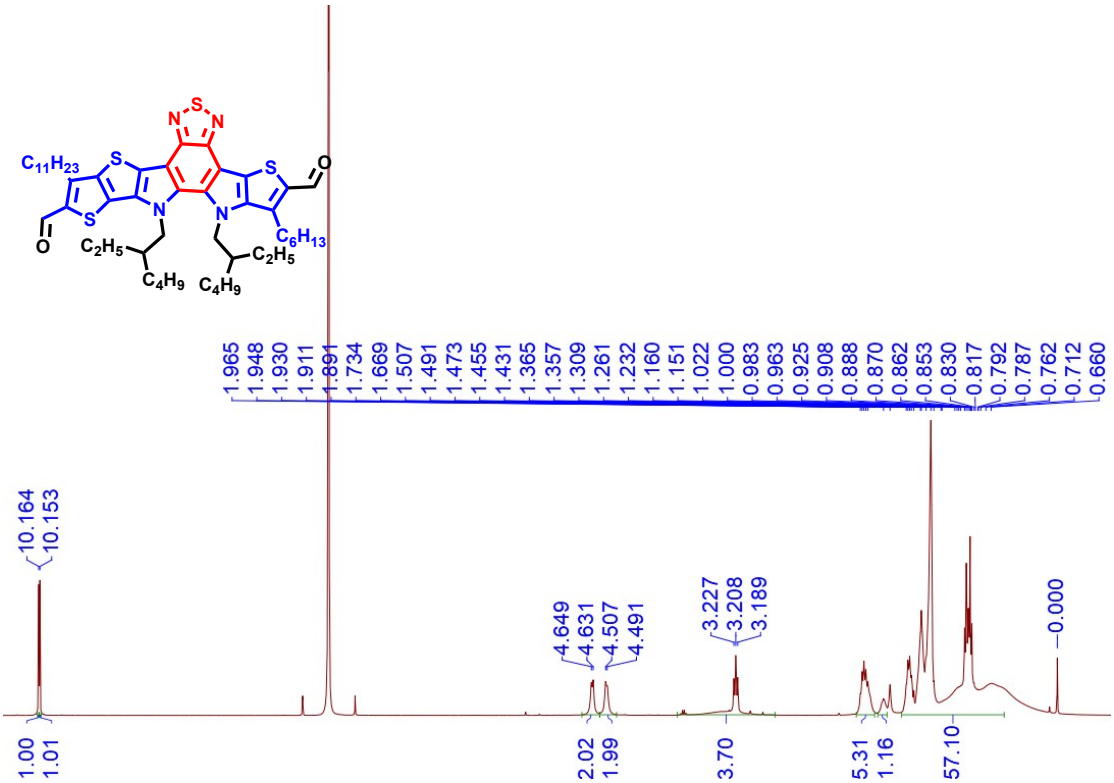

Fig. S12 The ^{1}H NMR spectrum of **Compound 5** in $CDCl_3$.

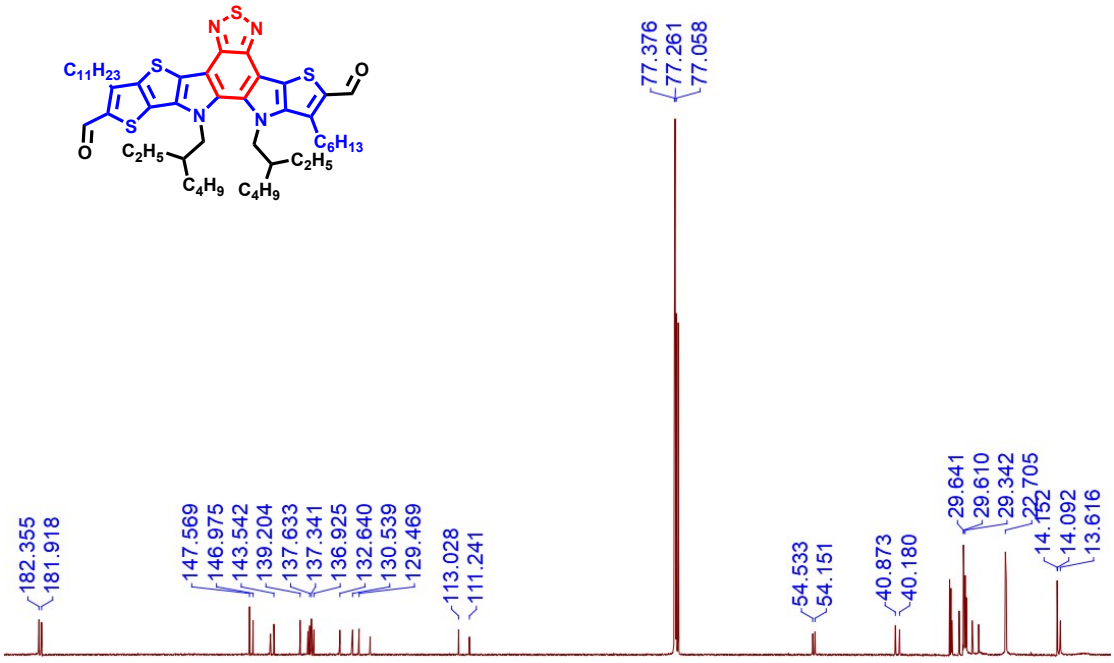

Fig. S13 The ^{13}C NMR spectrum of **Compound 5** in $CDCl_3$.

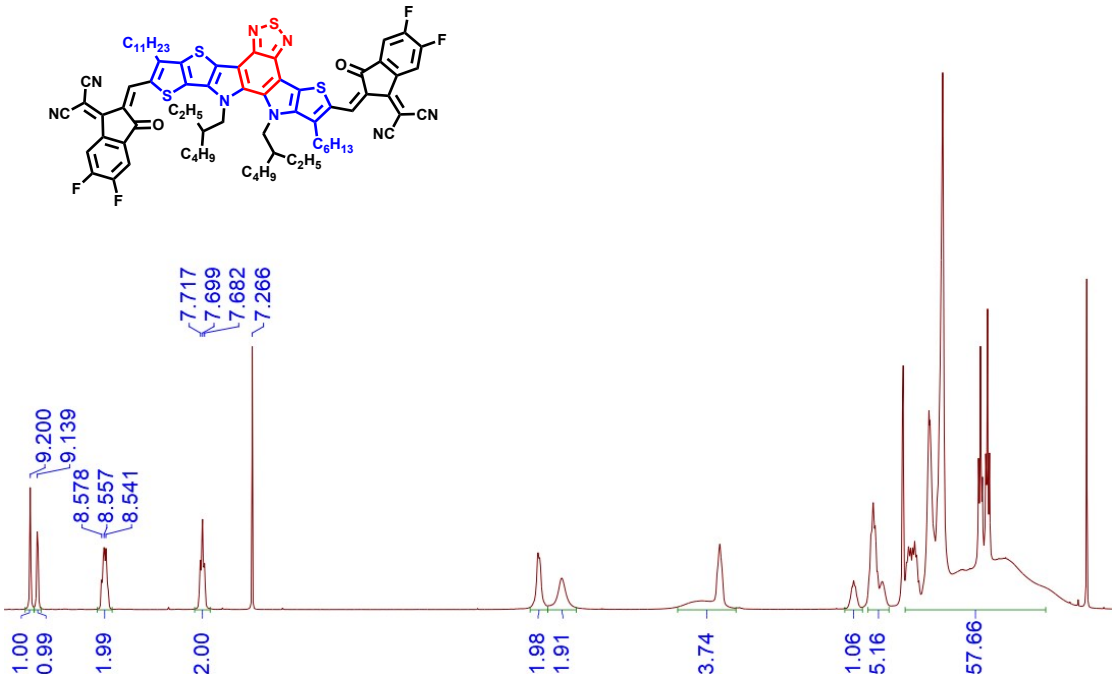

Fig. S14 The ^{1}H NMR spectrum of **AY6** in $CDCl_3$.

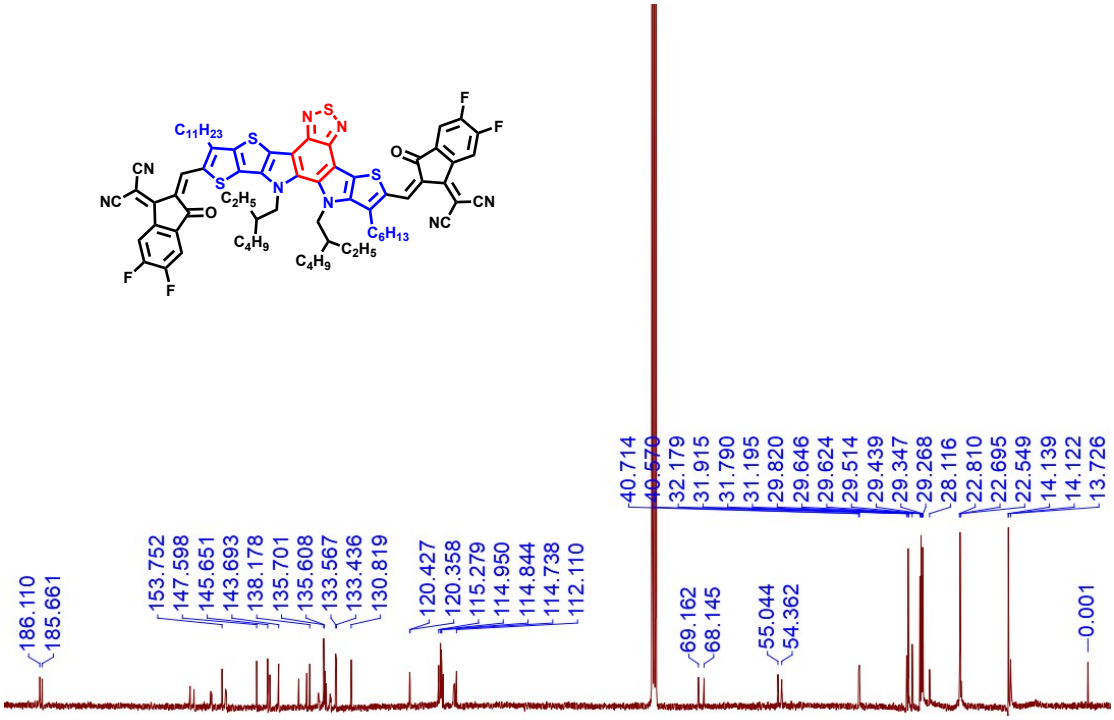

Fig. S15 The ^{13}C NMR spectrum of **AY6** in $CDCl_3$.

References

[1] W. Gao, M. Zhang, T. Liu, R. Ming, Q. An, K. Wu, D. Xie, Z. Luo, C. Zhong, F. Liu, F. Zhang, H. Yan and C. Yang, *Adv. Mater.* **2018**, *30*, 1800052.

[2] J. Yuan, Y. Zhang, L. Zhou, G. Zhang, H.-L. Yip, T.-K. Lau, X. Lu, C. Zhu, H. Peng, P. A. Johnson, M. Leclerc, Y. Cao, J. Ulanski, Y. Li, Y. Zou, *Joule* **2019**, *3*, 1140.

[3] H. Cha, D. S. Chung, S. Y. Bae, M. J. Lee, T. K. An, J. Hwang, K. H. Kim, Y. H. Kim, D. H. Choi, C. E. Park, *Adv. Funct. Mater.* **2013**, 23, 1556.

[4] S. Y. Chang, H. C. Liao, Y. T. Shao, Y. M. Sung, S. H. Hsu, C. C. Ho, W. F. Su, Y. F. Chen, *J. Mater. Chem. A.* **2013**, 1, 2447.

[5] Y. Zhang, D. Deng, K. Lu, J. Zhang, B. Xia, Y. Zhao, J. Fang, Z. Wei, *Adv. Mater.* **2015**, 27, 1071.

[6] F. Chen, G. Ding, A. Tang, B. Xiao, J. Li, E. Zhou, *J. Mater. Chem. C* **2018**, *6*, 2580.

[7] Y. Yin, J. Song, F. Guo, Y. Sun, L. Zhao, Y. Zhang, *ACS Appl. Energy Mater.* **2018**, *1*, 6577.

[8] W. Gao, M. Zhang, T. Liu, R. Ming, Q. An, K. Wu, D. Xie, Z. Luo, C. Zhong, F.

Liu, F. Zhang, H. Yan, C. Yang, *Adv. Mater.* **2018**, *30*, 1800052.

[9] J. Song, C. Li, L. Ye, C. Koh, Y. Cai, D. Wei, H. Y. Woo, Y. Sun, *J. Mater. Chem. A* **2018**, *6*, 18847.

[10] W. Gao, T. Liu, C. Zhong, G. Zhang, Y. Zhang, R. Ming, L. Zhang, J. Xin, K. Wu, Y. Guo, W. Ma, H. Yan, Y. Liu, C. Yang, *ACS Energy Lett.* **2018**, *3*, 1760.

[11] W. Gao, Q. An, C. Zhong, Z. Luo, R. Ming, M. Zhang, Y. Zou, F. Liu, F. Zhang, C. Yang, *Chem. Sci.* **2018**, *9*, 8142.

[12] C. Li, J. Song, L. Ye, C. Koh, K. Weng, H. Fu, Y. Cai, Y. Xie, D. Wei, H. Y. Woo, Y. Sun, *Sol. RRL* **2019**, *3*, 1800246.

[13] C. Li, T. Xia, J. Song, H. Fu, H. S. Ryu, K. Weng, L. Ye, H. Y. Woo, Y. Sun, *J. Mater. Chem. A* **2019**, *7*, 1435.

[14] L. Ye, Y. Xie, Y. Xiao, J. Song, C. Li, H. Fu, K. Weng, X. Lu, S. Tan, Y. Sun, *J. Mater. Chem. A* **2019**, *7*, 8055.

[15] T. J. Aldrich, M. Matta, W. Zhu, S. M. Swick, C. L. Stern, G. C. Schatz, A. Facchetti, F. S. Melkonyan, T. J. Marks, *J. Am. Chem. Soc.* **2019**, *141*, 3274.

[16] M. Li, Y. Zhou, J. Zhang, J. Song, Z. Bo, *J. Mater. Chem. A* **2019**, *7*, 8889.

[17] B. Gao, H. Yao, J. Hou, R. Yu, L. Hong, Y. Xu, J. Hou, *J. Mater. Chem. A* **2018**, *6*, 23644.

[18] J. Zhang, W. Liu, S. Chen, S. Xu, C. Yang, X. Zhu, *J. Mater. Chem. A* **2018**, *6*, 22519.

[19] W. Gao, T. Liu, R. Sun, G. Zhang, Y. Xiao, R. Ma, C. Zhong, X. Lu, J. Min, H. Yan, C. Yang, *Adv. Sci.* **2020**, *7*, 1902657.

[20] L. Yang, X. Song, J. Yu, H. Wang, Z. Zhang, R. Geng, J. Cao, D. Baran, W. Tang, *J. Mater. Chem. A* **2019**, *7*, 22279.